Volume 1 | Number 1 | Jan 2013 | Pages 1–100

Dalton Transactions

An international journal of inorganic chemistry
www.rsc.org/dalton

ROYAL SOCIETY OF CHEMISTRY

ROYAL SOCIETY OF CHEMISTRY

www.rsc.org/dalton

Dalton Transactions

ARTICLE

Three novel polyoxoanion-supported compounds: confinement of polyoxoanions in Ni-containing rigid concave surfaces with enhanced NLO properties

Yayu Dong, [a] Xiao Xu, [a] Guangpeng Zhou*,[b] Hao Miao, [a] GongHao Hu, [a] and Yan Xu *[a,c]

Three novel polyoxoanion-supported compounds modified by conjugate organic ligand tris(2-benzimidazylmethyl)amine (NTB) and nickel ions: $[Ni(NTB)(H_2O)]_2(H_2P_2Mo_5O_{23})\cdot9.25H_2O$ (**1**), $[Ni(H_2O)(NTB)]_2(PMo_{11}{}^{VI}Mo^VO_{40})\cdot4.5H_2O$ (**2**) and $[Ni(NTB)]_2(Mo_8O_{26})\cdot9H_2O$ (**3**) have been
10 successfully synthesized under hydrothermal conditions at different pH values. The compounds **1**-**3** contain the similar rigid concave surfaces $[Ni(NTB)]^{2+}$ cations, which connect with different clusters respectively to form the first examples of metal-NTB modified polyoxoanion-supported compounds. Transition metal-containing rigid concave surfaces masterly confine polyoxoanion in compounds **1**-**3**. In the synthesis of the three compounds, the pH values play an important role in the formation of
15 polyoxoanion and the stability of the compounds. Additionally, the third-order nonlinear optical properties (NLO) and electrochemical behaviors were also investigated.

Introduction

Polyoxometalates (POMs), as an attractive class of metal-oxygen
20 clusters, arouse increasing attentions not only because of their unmatched structural versatility, but also owing to their great potential applications in catalysis, magnetism, nonlinear optics, sensing and medicine.[1] The progress of polyoxometalates chemistry is always closely related to the functionalized POMs,
25 one of the vital area is making use of POMs' coordination abilities to synthesize polyoxoanion-supported or bridged transition metal complexes.[2] Because there are sufficient charge density and abundant oxygen atoms in the surface of the POMs, which make it more easily connect metal or metal complexes
30 together to form the new polyoxoanion-supported compounds. And the syntheses of these compounds have also greatly enriched material types of the POMs compounds.[3] In 2000, You's group first reported two Keggin unit supported by transition metal complexes, in which $[Ni(2,2´-bipy)_2(H_2O)]^{2+}$ and Keggin clusters
35 connected by covalent bonds.[4] Meanwhile, some polyoxoanion-supported compounds, including mono-supported,[5] bi-supported,[6] tri-supported[7] and tetra-supported[8] were reported. However, compared with classical polyoxometalates, the polyoxoanion-supported compounds were still less investigated.[9]
40 In the past decades, a major challenge in Host-guest chemistry has been study of globular molecules including fullerenes and carboranes confined by metal-containing rigid concave surfaces in the absence of electrostatic, hydrogen bonds and coordination interactions.[10] The shape of M-O cluster anions is globular, and
45 the size is also comparable with carboranes and fullerenes.

Therefore, it is vital to design M-O clusters confined by transition metal-containing rigid concave surfaces in order to explore their properties. We pay particular attention to conjugate host-guest complexes not only because of their characteristic aesthetic
50 architectures, but also more importantly due to their potential applications as functional materials in the nonlinear optical field. It is acknowledged that the strong conjugate structures could result in third-order NLO response. Presently, the researches of the POMs are mainly based on catalytic and magnetic
55 properties,[11] but reports on the nonlinear optical properties, especially third-order optical properties, are very rare. Take these into account, we intend to incorporate metal centers and organic concave surfaces materials into POMs to explore their nonlinear optical properties.[12] In the present work, we first employed NTB
60 (NTB = tris(2-benzimidazylmethyl)amine) as an conjugate organic ligand to make a rigid concave surface and introduced transition metal Ni^{2+} cations. Three new Ni-NTB modified polyoxoanion-supported compounds, $[Ni(NTB)(H_2O)]_2(H_2P_2Mo_5O_{23})\cdot9.25H_2O$ (**1**),
65 $[Ni(H_2O)(NTB)]_2(PMo_{11}{}^{VI}Mo^VO_{40})\cdot4.5H_2O$ (**2**) and $[Ni(NTB)]_2(Mo_8O_{26})\cdot9H_2O$ (**3**) with enhanced NLO properties have been successfully synthesized under hydrothermal conditions. Crystal structural analyses indicate that compounds **1**-**3** contain the similar rigid concave surface $[Ni(NTB)]^{2+}$ cations
70 and different polyoxoanions gathered as $[H_2P_2Mo_5O_{23}]^{4-}$, $[PMo_{11}{}^{VI}Mo^VO_{40}]^{4-}$ and $[Mo_8O_{26}]^{4-}$ clusters, respectively, which are masterly confined in the concave surface. The rigid concave surface $[Ni(NTB)]^{2+}$ cations confine polyoxoanions by various ways due to the different structures and symmetry of

polyoxoanions. To the best of our knowledge, compounds **1-3** represent the first examples of the M-NTB modified polyoxoanion-supported compounds. Additionally, the molecular TPA cross section σ of compounds **1-3** were calculated as 758,
5 404, and 673 GM (1 GM = 10^{-50} cm^{4}s / photon), respectively.

Experimental section

Materials and physical methods

NTB was prepared by following the known literature method,[13] other chemicals purchased were of reagent grade and used
10 without further purification. Elemental analyses (C, H, and N) were performed on a Perkin-Elmer 2400 elemental analyzer. IR spectra of compounds **1-3** were recorded with a Nicolet Impact 410 FTIR spectrometer with pressed KBr pellets from 4000 to 500 cm^{-1}. Single-crystal XRD data of **1-3** were obtained from a
15 Bruker Apex II CCD with Mo-Kα radiation (λ = 0.71073 Å) at 296K. Two-photon absorption (TPA) cross-sections (σ) were obtained by using Chameleon II femtosecond laser pulse and Ti: 95 sapphire system.

Preparation of [Ni(NTB)(H$_2$O)]$_2$(H$_2$P$_2$Mo$_5$O$_{23}$)·9.25H$_2$O (1)

20 A mixture of MoO$_3$ (0.0289 g, 0.2006 mmol), Ni(OAc)$_2$·4H$_2$O (0.0491 g, 0.1980 mmol), NTB (0.0407 g, 0.1035 mmol) was dissolved in 10 mL distilled water for 20 mins at room temperature. Then the pH of the mixture was adjusted to about 4.26 with H$_3$PO$_4$ (50 %), which was continuously stirred for 20
25 mins and then the suspension was put into a 25 mL Teflon-lined stainless-steel autoclave and kept under autogenous pressure at 125°C for 4.5 days. After slow cooling to room temperature, blue strip crystals were filtered and washed with distilled water (35 % yield based on Mo). Elemental analysis calc.: C, 28.17, H, 3.25,
30 N, 9.58%; found: C, 28.67, H, 2.84, N, 9.76%. IR (KBr, cm^{-1}): 3420 (vs), 1623 (m), 1473 (w), 1452 (m), 1384 (s), 1117 (m), 1055 (w), 1025 (w), 925 (s), 742 (m), 701 (s), 664 (w), 561 (w).

Preparation of [Ni(H$_2$O)(NTB)]$_2$(PMo$_{11}^{VI}$Mo^{V}O$_{40}$)·4.5H$_2$O (2)

A mixture of (NH$_4$)$_6$Mo$_7$O$_{24}$·4H$_2$O (0.1236 g, 0.1023mmol),
35 Ni(OAc)$_2$·4H$_2$O (0.0621 g, 0.2512 mmol), NTB (0.0207 g, 0.0526 mmol) was dissolved in 10 mL distilled water for 20 mins at room temperature. Then the pH of the mixture was adjusted to about 4 with H$_3$PO$_4$ (50 %) which was continuously stirred for 20 mins and then the suspension was put into a 25 mL Teflon-lined
40 stainless-steel autoclave and kept under autogenous pressure at 160 °C for 3 days. After slow cooling to room temperature, orange strip crystals were filtered and washed with distilled water (36 % yield based on Mo). Elemental analysis calc.: C, 20.07, H, 1.92, N, 6.83%; found: C, 20.06, H, 1.89, N, 6.83%. IR (KBr,
45 cm^{-1}): 3400 (vs), 1629 (m), 1472 (w), 1451 (w), 1377 (s), 1115 (w), 1051 (s), 960 (m), 873 (s), 807 (s), 738 (m), 627 (w).

Preparation of [Ni(NTB)]$_2$(Mo$_8$O$_{26}$)·9H$_2$O (3)

Compound **3** was obtained by using the same procedure as described for compound **2**, but the pH of the mixture was
50 adjusted to about 2 with 2M HNO$_3$ and kept under autogenous pressure at 120 °C for 3 days. Green strip crystals of compound 3 were obtained (41% yield based on Mo). Elemental analysis calc.: C, 25.31, H, 2.63, N, 8.60%; found: C, 26.01, H, 2.45, N, 9.16%. IR (KBr, cm^{-1}): 3390 (vs), 1637 (s), 1456 (w), 1388 (s), 1160 (w),

55 1112 (m), 1046 (w), 955 (w), 915 (w), 758 (w), 708 (w), 670 (w).

X-Ray crystallography

The collection of single-crystal X-ray analyses data were performed on a Bruker Apex II CCD equipped with a normal focus at 296K, sealed tube X-ray source (Mo-Kα radiation, λ =
60 0.71073 Å) operating at 50 kV and 30 mA. The structures were solved by direct methods and refined by full-matrix least-squares using the SHELXL-2014/7 program package. Anisotropic thermal parameters were used to refine all non-hydrogen atoms. A summary of the crystallographic data and structure
65 determination for the three compounds is provided in Table 1. Selected bond lengths for compounds **1-3** are given in Table SI1-SI3†. Distances (Å) and angles (°) of hydrogen bonds for compounds **1-3** are given in Table SI4-SI6†.

Table 1. Crystal data and structure refinements for compounds **1-3**

Compounds	**1**	**2**	**3**
Formula	C$_{48}$H$_{66.5}$Mo$_5$N$_{14}$Ni$_2$O$_{34.25}$P$_2$	C$_{48}$H$_{55}$Mo$_{12}$N$_{14}$Ni$_2$O$_{46.5}$P	C$_{48}$H$_{60}$Mo$_8$N$_{14}$Ni$_2$O$_{35}$
Fw	2046.71	2871.73	2278.04
T (K)	296(2)	296(2)	296(2)
Wavelength (Å)	0.71073	0.71073	0.71073
Crystal system, space group	Monoclinic P2$_1$ / n	Monoclinic P2$_1$	Triclinic P-1
a (Å)	10.4981(8)	13.907(2)	10.787(8)
b (Å)	35.614(3)	24.215(4)	12.279(9)
c (Å)	19.4718(15)	24.310(4)	15.855(11)
α (°)	90	90	91.471(9)
β (°)	94.6820(10)	101.604(2)	104.183(9)
γ (°)	90	90	110.064(8)
V (Å^3)	7255.9(10)	8020(2)	1899(2)
Z	4	4	1
Dc (Mg / m^3)	1.874	2.378	1.992
μ (mm^{-1})	1.485	2.390	1.851
F(000)	4090	5552	1118
Crystal size (mm^3)	0.17 x 0.13 x 0.12	0.17 x 0.14 x 0.12	0.15 x 0.13 x 0.12
Limiting indices	-12 ≤ h ≤ 12 -43 ≤ k ≤ 42 -23 ≤ l ≤ 23	-16 ≤ h ≤ 16 -28 ≤ k ≤ 29 -29 ≤ l ≤ 29	-12 ≤ h ≤ 12 -13 ≤ k ≤ 14 -18 ≤ l ≤ 18
Reflections collected	53015	58856	13583
Independent reflection	13431 [R(int) = 0.0554]	26620 [R(int) = 0.0468]	6620 [R(int) = 0.0451]
Completeness	99.70%	99.80%	98.90%
Refinement method	Full-matrix least-squares on F^2	Full-matrix least-squares on F^2	Full-matrix least-squares on F^2
Data/restraints/parameters	13431/85/997	26620/20/2235	6620/50/505
Goodness-of-fit on F^2	1.103	1.037	1.010
Final R indices [I > 2sigma(I)]	R$_1$ = 0.0419, wR$_2$=0.1040	R$_1$ = 0.0428, wR$_2$=0.0946	R$_1$ = 0.0468, wR$_2$= 0.1164

[a] $R_1 = \Sigma\|F_o| - |F_c\|/\Sigma|F_o|$. [b] $wR_2 = \Sigma[w(F_o^2 - F_c^2)^2]/\Sigma[w(F_o^2)^2]^{1/2}$.

Results and discussion

Synthesis

Hydrothermal synthesis has recently been proven to be a particularly powerful method in the synthesis of polyoxoanion-supported compounds. During a specific hydrothermal synthesis, there are many factors can affect the nucleation and crystal growth of final products, such as reactants, concentrations of reactants, solvents and temperatures, reaction time, pH values, in which pH values play an important role in the formation of these structures.[14] In the syntheses of compounds **1-3**, MoO_3, $(NH_4)_6Mo_7O_{24}\cdot4H_2O$, NTB and $Ni(OAc)_2\cdot4H_2O$ were used as starting reactants, and excess H_3PO_4 or HNO_3 was added. The effect of acids is not only to ensure to provide the required amounts of P with compounds **1** and **2**, but also to control the pH values.[15] Compared with **2**, the cluster $[H_2P_2Mo_5O_{23}]^{4-}$ in **1** was obtained in the higher pH (4.26), while lower pH (4.0) favored Keggin structure under hydrothermal conditions, which is similar to the literature.[16] In the synthesis of compounds **2**, the $[PMo_{11}^{VI}Mo^VO_{40}]^{4-}$ was obtained under the environment of H_3PO_4, while cluster anion $[Mo_8O_{26}]^{4-}$ in **3** was generated under the environment of HNO_3 (pH = 2.0). The synthesis of three compounds indicates that the pH and acids play crucial roles in the formation of compounds **1-3**.

Description of the Structures

Crystal structure of 1

Single-crystal X-ray diffraction analysis revealed that compound **1** consists of two principal structural building units (SBUs): $[H_2P_2Mo_5O_{23}]^{4-}$ anion (SBU-1) and rigid concave surfaces $[Ni(NTB)]^{2+}$ cations (SBU-2). SBU-1 can be viewed as a ring of five distorted MoO_6 octahedra with two capped PO_4 tetrahedra on each side (Fig. SI1†).[17] Each phosphate subunit shares three oxo-groups with the molybdate ring. One of these oxo-groups is μ_2-bridging, linking one molybdenum site and the phosphorus while the others adopt a μ_3-bridging mode, linking two molybdenum sites and the phosphorus. The VB-Calculations indicate that O17 and O20 of PO_4 tetrahedron are mono-protonated (Table S7). P-O and Mo-O distances are in the ranges of 1.505(4)-1.575(4) Å and 1.691(3)-2.403(3) Å, respectively. SBU-2 contain two crystallographically independent Ni atoms, whose coordination environments are entirely similar and coordinated by four N atoms from different NTB ligands, one oxygen atom from a MoO_6 octahedron group and one oxygen atom of the coordinated water (Fig 1b). Ni-O and Ni-N distances are in the ranges of 2.054(3)-2.152(4) Å and 2.012(4)-2.201(4) Å. The above bonds length data are consonant with reported in the literatures.[18] $[H_2P_2Mo_5O_{23}]^{4-}$ anion connects two $[Ni(NTB)]^{2+}$ units in the opposite two sides by single Ni-O bond. Meanwhile, $[H_2P_2Mo_5O_{23}]^{4-}$ anion is successfully confined by the concave surfaces (Fig 1c). Interestingly, $[Ni(NTB)]^{2+}$ cations can be regarded as two hands that hold polyoxoanion.
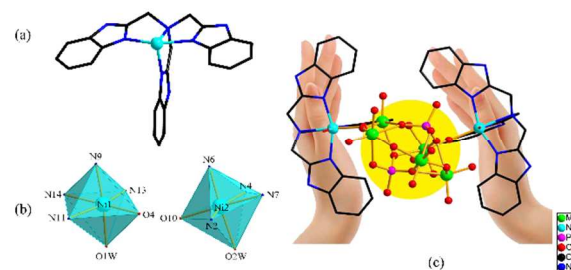

Fig. 1 (a) The structure of SBU-2; (b) The coordination environment of Ni^{2+}; (c) P_2Mo_5 anion is confined by the rigid concave surface of $[Ni(NTB)]^{2+}$ cations.

It's worth noting that compound **1** possess both hydrogen bonds and π-π stacking interactions (3.847 Å) between the adjacent clusters, which greatly enhance stability of the structure. Through extend hydrogen bonds (Table S4), π-π stacking interaction interacts together to give a 3D supramolecular network (Fig 2). It can be seen that the hydrogen bonds and π-π stacking interactions play a key role in building up and stabilizing solid frameworks.[19]
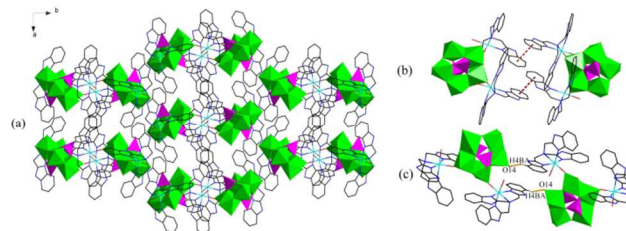

Fig. 2 (a) Polyhedral representation of the 3D framework of compound **1** along the c-axis; The π-π stacking (b) and hydrogen bonding interactions (c) in compound **1**.

Crystal Structure of 2

The asymmetric unit of compound **2** also consists two principal SBUs: $[PMo_{11}^{VI}Mo^VO_{40}]^{4-}$ anion (SBU-1) and rigid concave surfaces $[Ni(NTB)]^{2+}$ cations (SBU-2). SBU-1 is the well-known α-Keggin-type structures that possess one PO_4 tetrahedron and twelve MoO_6 octahedra. PO_4 tetrahedron is located in the center of the structure, while MoO_6 octahedra connect PO_4 tetrahedron to form the Keggin structure by corner-sharing and edge-sharing manner (Fig. SI2†). P-O and Mo-O distances of compound **2** fall into the ranges of 1.511(6)-1.548(5) Å and 1.647(7)-2.506(6) Å, which are in close agreement with those reported POM-based compounds.[20] Bond valence sum (BVS) calculations indicates that eleven molybdenum atoms are in the +6 oxidation states and the remaining one is in the +5 oxidation states in PMo_{12} clusters. The coordination environments of Ni atoms in SBU-2 are similar to compound **1**, which are chelated by four nitrogen atoms from one NTB ligand, one oxygen atom from a MoO_6 octahedron group of the PMo_{12} cluster and one oxygen atom of the coordinated water molecule. The bond lengths of Ni-O and Ni-N are in the ranges of 2.057(5)-2.151(7) Å and 2.000(8)-2.187(7) Å, respectively. PMo_{12} anion also connects the $[Ni(NTB)]^{2+}$ cations by single Ni-O band. It's worth noting that the shape and size of PMo_{12} cluster is similar with fullerene and bigger than P_2Mo_5 and Mo_8 clusters, so that the rigid concave surface confine PMo_{12} in a different manner. It is cupped in hands rather than between two hands. Compared to compound **1**, compound **2** yield 3D supramolecular networks only by hydrogen bonds (C-H···O, N-

H···O) as shown in Fig 4a. It is worth reminding that there are a variety of hydrogen bonds between adjacent clusters, which greatly enhance the stability of the structure (Fig 4b).
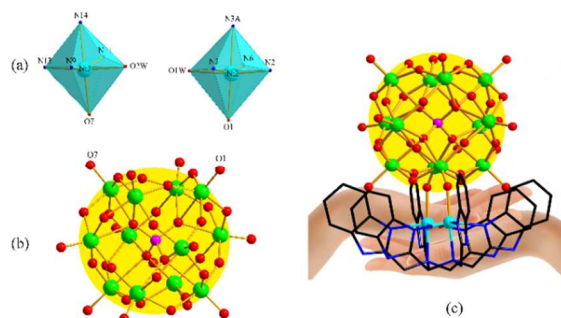

5 **Fig. 3** (a) The coordination environment of Ni^{2+} and (b) ball-and-stick representation of the Keggin structural anion and gold ball as the background is the abstract view of the anion. (c) PMo_{12} anion is confined by the rigid concave surface of $[Ni(NTB)]^{2+}$ cations.
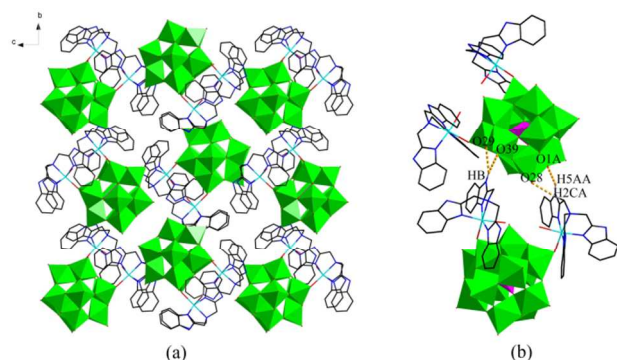

10 **Fig. 4** (a) The 3D framework of compound **2** along the a-axis; (b) hydrogen bonding interactions in compound **2**

Crystal Structure of 3

The structure of compound **3**, similar to compounds **1** and **2**, also consists of two principal SBUs: $[Mo_8O_{26}]^{4-}$ anion (SBU-1) and 15 rigid concave surfaces $[Ni(NTB)]^{2+}$ cations (SBU-2) (Fig 5). The octamolybdate anion Mo_8 is well characterized in the literature with α-η isomers,[21] and in compound **3**, octamolybdate is in its β form (Fig. SI3†). The β-octamolybdate is composed of eight edge-sharing MoO_6 octahedra, out of which six octahedra are 20 characterized by two terminal oxygen atoms (O_t) attached to each Mo atom and each of the remaining two MoO_6 octahedra has one O_t. Overall, the cluster consists of six μ_2-oxygen (O_b) atoms, four μ_3-oxygen (O_b) atoms and two μ_4-oxygen (O_b) atoms along with the terminal oxygen atoms. The coordination environments of Ni 25 atoms are similar to compounds **1** and **2**, except one oxygen atom from MoO_6 octahedron group instead of coordinated water molecule. The bonds lengths between Ni-O and Ni-N are in the ranges of 2.031(4)-2.183(4) Å and 2.007(5)-2.191(4) Å, which are in good accordance with the literatures.[22] However, different 30 from compounds **1** and **2**, Mo_8 links to each $[Ni(NTB)]^{2+}$ cation by double Ni-O bands, which is also successfully confined by the hands shape concave surface. The 3D supramolecular network of compound **3** is also formed only by hydrogen bonds (Fig 6, Table s6).
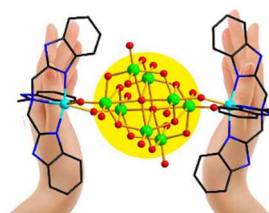

35 **Fig. 5** Mo_8 anion is confined by the rigid concave surface of $[Ni(NTB)]^{2+}$.
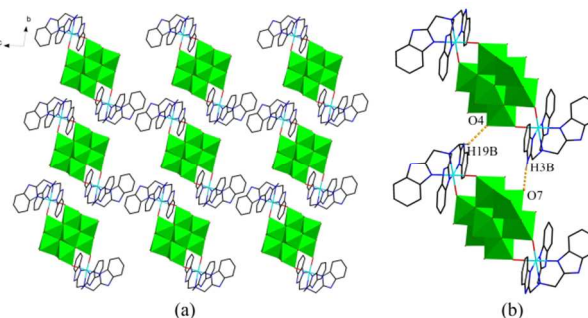

Fig. 6 (a) The 3D framework of compound 3 along the a-axis; (b) hydrogen bonding interactions between adjacent clusters

40 Compared with other inorganic-organic hybrid polyoxometalates[23], compounds **1-3** are very different. Compounds **1-3** contain the similar rigid concave surfaces $[Ni(NTB)]^{2+}$ cations, which further connected different polyoxoanions by Ni-O bonds to construct the first examples of 45 metal-NTB modified polyoxoanion-supported compounds. Interestingly, $[Ni(NTB)]^{2+}$ cations can be described as two hands and masterly confine polyoxoanions in concave surfaces. Additionally, the different structures and size of polyoxoanions lead to various locating position of hands in three compounds.

50 ### Powder X-ray diffraction

PXRD measurements for compounds **1-3** were determined at room temperature (Fig SI4 and SI5†), diffraction peak positions of the experimental PXRD patterns of **1-3** are in agreement with those of the simulated PXRD patterns, which indicate the phase 55 purity of compounds **1-3**.

IR spectra

The IR spectra of compounds **1-3** were recorded between ν = 4000-500 cm^{-1} (Fig SI6 and SI7†), which display the stretching 60 vibration peaks. Characteristic vibration patterns of the ν(Mo-O-Mo) are in the 701, 742 cm^{-1} (**1**), 741, 808 and 876 cm^{-1} (**2**) and 670, 708 and 758 cm^{-1} (**3**). The peaks at 930 cm^{-1} (**1**), 960 cm^{-1} (**2**) and 962 cm^{-1} (**3**) could be associated with the ν(Mo=O) vibration, and 1055 cm^{-1} (**1**), 1051 cm^{-1} (**2**) could be ascribed to ν(P-O). The 65 characteristic adsorption bands of the NTB ligands are observed in the range of 1117-1623 cm^{-1} (**1**), 1115-1629 cm^{-1} (**2**), 1112-1637 cm^{-1} (**3**), whereas the characteristic adsorption bands of the water molecules appear at 3420 cm^{-1} (**1**), 3400 cm^{-1} (**2**), 3390 cm^{-1} (**3**), respectively. The occurrence of these characteristic 70 adsorption bands is consistent with the similar compounds in the reported literatures.[24]

Two-photon Absorption

NTB is exactly an excellent strong conjugate organic ligand and

the combination of POMs with NTB can give rise to a strong NLO response. Herein we studied the third-order NLO properties of three M-NTB modified polyoxoanion-supported compounds. The open-aperture Z-scan experiments revealed that the third-order NLO properties of compounds **1**-3 in DMF at a concentration of 1.0×10^{-3} mol·L^{-1}. Two-photon absorption (TPA) values containing TPA coefficient β and TPA cross section σ were measured by the open-aperture Z-scan technique with femtosecond laser pulse and Ti:95 sapphire system. Fig 7 and 8 show the open aperture Z-scan curves of compounds **1**-3, respectively. The red unfilled circles are the experimental data and the blue line represents the theoretical simulated curve modified by the following equations: (1) and (2). And as show in Figs, the normalized transmittance curve has an obvious peak valley near the focus z = 0 in the three compounds, which show significant nonlinear absorption characteristics.

$$T(z, s=1) = \sum_{m=0}^{\infty} \frac{[-q_0(z)]^m}{(m+1)^{3/2}} \quad \text{for } |q_0| < 1 \tag{1}$$

$$q_0(z) = \frac{\beta I_0 L_{eff}}{1 + z^2 / z_0^2} \tag{2}$$

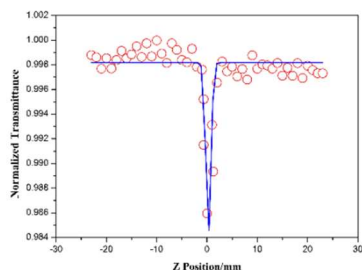**Fig. 7** The open aperture z-scan data at 720 nm for compound **1** in DMF at 1.0×10-3 mol L^{-1}

where β is the TPA cofficient of the solution, I_0 is the input intensity of laser beam at the focus z = 0, $L_{eff} = (1 - e^{-\alpha L})/\alpha$ is the effective length with α and L are the linear absorption coefficient and the sample length respectively. z is the sample position, $z_0 = \pi \omega_0^2 / \lambda$ is the diffraction length of the beam, in which the ω_0 and λ are the spot size at the focus and the wavelength of the beam respectively. By using the equations mentioned above, we deduce the TPA absorption coefficient β are calculated as 0.001655, 0.001127 and 0.015925 cm / GW for compounds **1**-3. Furthermore, the molecular TPA cross section σ can be calculated by the following relationship:
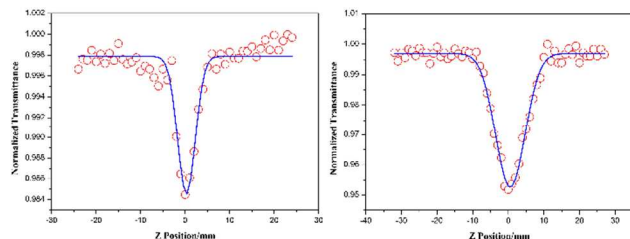
$$\sigma N_A d \times 10^{-3} = h \nu \beta \tag{3}$$

Fig. 8 The open aperture z-scan data at 920 nm for compound **2** (Left) and 780 nm for compound **3** (Right) in DMF at 1.0×10^{-3} mol L^{-1}

where N_A, d, h and v are respectively the Avogadro's constant, the

concentration of the compound, the Planck's constant and the frequency of input intensity. Based on Eq. (3)[25], the molecular TPA cross section σ of compounds **1**-3 were calculated as 758, 404 and 673 GM (1 GM = 10^{-50} cm^{4}s / photon), respectively. To our knowledge, compound **1** has the biggest molecular TPA cross section σ comparing with other POM-based NLO materials[14,26]. The third-order NLO property of compounds **1**-3 indicate that the combination of POMs with NTB give rise to a strong NLO response, which may be a good choice of NLO materials.

Cyclic Voltammetric Behaviors of Compounds 1-3

The electrochemical behaviors of compounds **1**-3 were studied in 1 mol / L H$_2$SO$_4$ solution at changing scanning speeds, which depend on the different electrochemical behaviors of parent $[H_2P_2Mo_5O_{23}]^{4-}$, $[PMo_{11}^{VI}Mo^VO_{40}]^{4-}$ and $[Mo_8O_{26}]^{4-}$ polyoxoanions. From −100 to 600 mV for compounds **1** (Fig 9) and **2** (Fig 10), while range of -200 mV to 1500 mV for compound **3** (Fig 10), three pairs of reversible peaks related to oxidation-reduction reactions are detected. The average peak potentials E$_{1/2}$ = (Epa + Epc) / 2 of I/I′, II/II′, and III/III′ are −88, 200 and 345 mV for compound **1**, −167, 209 and 367 mV for compound **2** as well as -48, 198 and 399 mV for compound **3**, respectively. These pairs of redox peaks should be ascribed to three consecutive double electronic reduction processes of Mo centers.[27] In addition, the cathodic peaks move to the negative potentials values, whereas the corresponding anodic peaks shift towards the positive potentials values and the peak potentials also vary progressively when enhancing scanning speed from 50 to 350 mV s^{-1} for compound **1**, 50 to 450 mV·s^{-1} for compound **2** and 50 to 400 mV·s^{-1} for compound **3**. The results exhibit almost no structure effect on the redox properties, except for some potential shifts of the redox peaks, confirming the electrochemical stability and robustness of the method used to prepare the modified electrodes. The results also d show that these Ni-NTB modified polyoxoanion-supported compounds have a potential application in electrochemistry.
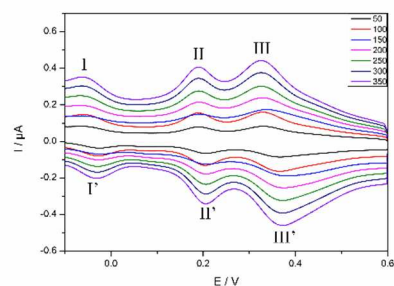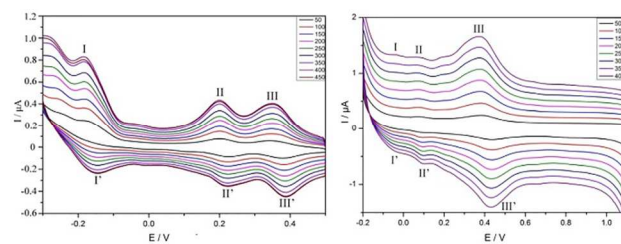

Fig. 9 The CV curve of compound **1**

Fig. 10 The CV curves of compounds **2** (Left) and **3** (Right)

Conclusions

In conclusion, we successfully synthesized three Ni-NTB modified polyoxoanion-supported compounds. Compounds **1-3** contain the similar rigid concave surfaces $[Ni(NTB)]^{2+}$ cations, which masterly confine polyoxoanions in concave surfaces. Meaningfully, they reprsent the first examples of the polyoxoanion-supported modified by the concave surfaces Ni-NTB. The different self-assembly of compounds **1-3** demonstrate that the pH values have a great influence on the final structures. Additionally, these compounds have modest molecular TPA cross section σ; therefore they have potential applications in the fields of nonlinear optics. It is reasonable to believe that the synthetic strategy of this work might be a significant step towards the design and synthesize new functional hybrid materials based on POMs.

Supplementary data

CCDC- 1412098 -1412100 contain the supplementary crystallographic data for compound **1** and **2**. These data can be obtained free of charge via http://www.ccdc.com.ac.uk/conts/retrieving.html,or from Cambridge Crystallographic Data Centre, 12 Union Road, Cambridge CB2 1E2, UK; fax: (+44) 1223-336-033; or e-mail: deposit@ccdc.cam.ac.uk

Acknowledgements

Notes and references

[a] *College of Chemistry and Chemical Engineering, State Key Laboratory of Materials-Oriented Chemical Engineering, Nanjing Tech University, Nanjing 210009, PR China. E-mail: yanxu@njtech.edu.cn*
[b] *College of Chemistry and Chemical Engineering, Chongqing University of Technology, Chongqing 400054, P. R. China. E-mail: gpzhou@cqut.edu.cn*
[c] *Coordination Chemistry Institute, State Key Laboratory of Coordination Chemistry, Nanjing University, Nanjing 210093, PR China*

†Electronic supplementary information (ESI) available: PXRD patterns, IR spectra, selected bond distances and angles, hydrogen bond interactions of **1-3**. CCDC . For ESI and crystallographic data in CIF or other electronic format, see DOI:xxxxx

1 V. Artero, A. Proust, P. Herson, F. Villain, C. Cartier dit Moulin, P. Gouzerh, *J. Am. Chem. Soc.*, 2003, **125**, 11156; C. L. Hill, G. C. White, *Chem. Rev.*, 1998, **98**, 1; J. M. Clemente-Juan, E. Coronado, A. Gaita-Arino, *Chem. Soc. Rev.*, 2012, **41**, 7464; D. L. Long, R. Tsunashima, L. Cronin, *Angew. Chem. Int. Ed.*, 2010, **49**, 1736; X. L. Wang, C. Qin, E. B. Wang, Z. M. Su, Y. G. Li, L. Xu, *Angew. Chem. Int. Ed.*, 2006, **45**, 7411; D. E. J. Katsoulis, *Chem. Rev.*, 1998, **98**, 359; X. Xu, W. W. Ju, W. T. Hou, D. R. Zhu, Y. Xu, *CrystEngComm*, 2014, **16**, 82.

2 C. X. Zhang, Y. G. Chen, Q. Tang, Z. C. Zhang, D. D. Liu, H. X. Meng, *Inorg. Chem. Commun.*, 2012, **17**, 155.

3 Q. Guo, C. Xu, B. Zhao, Y. Jia, H. Hou, Y. Fan, *Cryst. Growth Des.*, **2012**, **12**, 5439; K. H. He, Y. W. Li, Y. Q. Chen, W. C. Song, X. H. Bu, *Crytl. Growth Des.*, 2012, **12**, 2730; C. Jahier, S. Nlate, *Eur. J. Inorg. Chem.*, 2012, **5**, 833; Y. Q. Jiao, C. Qin, C. Y. Sun, K. Z. Shao, P. J. Liu, P. Huang, Z. M. Su, *Inorg. Chem. Commun.*, 2012, **20**, 273.

4 Y. Xu, K. L. Zhang, Y. Zhang, X. Z. You, J. Q. Xu, *Chem. Commun.*, 2000, **2**, 153.

5 J. Y. Niu, Z. L. Wang, J. P. Wang, *Inorg. Chem. Commun.*, 2003, **6**, 1272; Y. Lu, Y. Xu, E. B. Wang, J. Lü, C. W. Hu, L. Xu, *Cryst. Growth Des.*, 2005, **5**, 257.

6 M. Yuan, Y. G. Li, E. B. Wang, C. G. Tian, L. C Wang, W. Hu, N. H. Hu, H. Q. Jia, *Inorg. Chem.*, 2003, **42**, 3670; C. M. Liu, D. Q. Zhang, D. B. Zhu, *Cryst. Growth Des.*, 2003, **3**, 363; Shi, Z. Yu.; Gu, X. J. Peng, J. Chen, Y. H. *J. Solid State Chem.*, 2005, **178**, 1988.

7 Y. K. Lu, X. B. Cui, Y. Chen, J. N. Xu, Q. B. Zhang, Y. B. Liu, J. Q. Xu, T. G. Wang, J. Solid State Chem., 2009, **182**, 2111; J. W. Cui, X. B. Cui, J. N. Xu, H. H. Yu, J. Q. Xu, W. J. Duan, T. G. Wang, *J. Mol. Struct.*, 2008, **891**, 35.

8 Y. Lu, Y. G. Li, E. B. Wang, X. X. Xu, Y. Ma, *Inorg. Chim. Acta.*, 2007, **360**, 2063-2070; S. Reinoso, P. Vitoria, L. Lezama, A. Luque, J. M. GutierrezZorrilla, *Inorg. Chem.*, 2003, **42**, 3709; X. G. Cao, L.W. He, B. Z. Lin, Z. J. Chen, P. D. Liu, *Inorg. Chim. Acta.*, 2009, **362**, 2505.

9 Q. Zhang, H. Zhang, S. Zeng, D. Sun, C. Zhang, *Asian. J. Chem.*, 2013, **8**, 1985; D. D. Zhang, Y. H. Zhang, J. Zhao, P. Ma, J. P. Wang, J. Y Niu, *Eur. J. Inorg. Chem.*, 2013, **2013**, 1672; Y. Zheng, Q. C. Zhang, L. S. Long, R. B. Huang, A. Müller, J. Schnack, Z. S. Zheng, Z. P. Zheng, *Chem. Commun.*, 2013, **49**, 36.

10 P. C. Andrews, J. L. Atwood, L. J. Barbour, P. J. Nichols and C. L. Raston, *Chem.-Eur. J.*, 1998, **4**, 1384; P. D. Croucher, J. M. Marshall, P. J. Nichols, C. L. Raston, *Chem. Commun.*, 1999, 193; J. Fu, H. X. Sun, Y. Xu, C. L Wang, D. R Zhu, Q. Sun, H. K. Liu, *CrystEngComm*, 2012, **14**, 5148.

11 H. Lv, W. Guo, K. Wu, Z. Chen, J. Bacsa, D. G. Musaev, C. L. Hill, *J. Am. Chem. Soc.*, 2014, **136**, 14015; J. W. Vickers, H. Lv, J. M. Sumliner, G. Zhu, Z. Luo, D. G. Musaev, C. L. Hill, *J. Am. Chem. Soc.*, 2013, **135**, 14110; X. B. Han, Z. M. Zhang, T. Zhang, Y. G. Li, W. Lin, W. You, E. B. Wang, *J. Am. Chem. Soc.*, 2014 **136**, 5359; J. W. Vickers, H. Lv, J. M. Sumliner, G. Zhu, Z. Luo, D. G. Musaev, C. L. Hill, *J. Am. Chem. Soc.*, 2013.**135**, 14110.

12 W. H. Zhang, Y. L. Song, Y. Zhang, J. P. Lang, *Cryst. Growth Des.*, 2007, 8, 253; Z. H. Wei, C. Y. Ni, H. X. Li, Z. G. Ren, Z. R. Sun, J. P. Lang, *Chem. Commun.*, 2013, **49**, 4836.

13 M. M. Ibrahim, M. A. Amin, *J. Mol. Struct.*, 2011, **985**, 191.

14 H. Miao, H. X. Wan, M. Liu, Y. Zhang, X. Xu, W. W. Ju, Y. Xu, *J. Mater. Chem. C*, 2014, **2**, 6554.

15 Z. L. Li, Y. Wang, L. C. Zhang, J. P. Wang, W. S. You, Z. M. Zhu, *Dalton Trans.*, 2014, **43**, 5840.

16 K. Yu, B. B. Zhou, Y. Yu, Z. H. Su, H. Y. Wang, C. M. Wang, C. X. Wang, *Dalton Trans.*, 2012, **41**, 10014; J. Y. Niu, J. C. Ma, J. W. Zhao, P. T. Ma, J. P. Wang, *Inorg. Chem. Commun.*, 2011, **14**, 474.

17 X. M. Lu, X. J. Wang, P. Z. Li, X. H. Pei, C. H. Ye, *J. Mol. Struct.*, 2008, **872**, 129.

18 Q. G. Zhai, X. Y. Wu, S. M. Chen, L. J. Chen, C. Z. Lu, *Inorg. Chim. Acta.*, 2007, 360, 3484; H. L. Chen, M. X. Li, X. He, Z. X. Wang, M. Shao, S. R. Zhu, *Inorg. Chim. Acta.*, 2010, **363**, 3186.

19 H. J. Jin, B. B. Zhou, Y. Yu, Z. F. Zhao, Z. H. Su, *CrystEngComm*, 2011, **13**, 585.

20 K. Yu, B. B. Zhou, Y. Yu, Z. H. Su, C. M. Wang, C. X. Wang, S. Gao, Y. Chen, *Inorg. Chim. Acta.*, 2012, **384**, 8; R. Khoshnavazi, L. Bahrami, H. Davoodi, *Inorg. Chim. Acta.*, 2012, **382**, 158.

21 T. Arumuganathan, S. K. Das, *Inorg. Chem.*, 2009, **48**, 496.

22 L. Luo, H. Lin, L. Li, T. I. Smirnova, P. A. Maggard, *Inorg. Chem.*, 2014, **53**, 3464-3470; X. B. Cui, K. Lü, Y. Fan, J. Q. Xu, L. Ye, Y. H. Sun, Z. H. Yi, *J. Mol. Struct.*, 2005, **743**, 151; F. X. Meng, Y. G. Chen, H. B. Liu, H. J. Pang, D. M. Shi, Y. Sun, *J. Mol. Struct.*, 2007, **837**, 224.

23 L. Yuan, C. Qin, X. L. Wang, Y. G. Li, E. B. Wang, *Dalton Trans.*, 2009, **21**, 4169; S. Chang, C. Qin, E. B. Wang, Y. G. Li, X. L. Wang, *Inorg. Chem. Commun.*, 2006, **9**, 727; D. Chandan, K. Tanay, B. Rahul, *Chem. Commun.*, 2012, **48**, 266; W. Q. Kan, S. Z. Wen, Y. H. Kan, H. Y. Hu, S. Y. Niu, X. Y. Zhang, *Synthetic Metals*, 2014.**198**, 51.

24 X. Z. Liu, B. Z. Lin, L. W. He, X. F. Huang, Y. L. Chen, *J. Mol. Struct.*, 2008, **877**, 72; H. H. Yu, X. B. Cui, J. Lu, Y. H. Sun, W. J.

Duan, J. W. Cui, T.G. Wang, *J. Mol. Struct.*, 2008, **879**, 156; P. P. Zhang, J. Peng, A. X. Tian, H. J. Pang, Y. Chen, M. Zhu, Y. H. Wang, *J. Mol. Struct.*, 2010, **968**, 19.

25 D. M. Li, Q. Zhang, P. Wang, J. Y. Wu, Y. H. Kan, Y. P. Tian, H. P.
5   Zhou, J. X. Yang, X. T. Tao, M. H. Jiang, *Dalton Trans.*, 2011, **40**, 8170; M. Sheik. Bahae, A. A. Said, T. H. Wei, D. J. Hagan, E. W. Van Stryland, *IEEE. J. Quantum Electron.*, 1990, **26**, 760; W. W. Ju, H. T. Zhang, X. Xu, Y. Zhang, Y. Xu, *Inorg. Chem.*, 2014, **53**, 3269.

26 Y. Zhang, L. Huang, H. Miao, H. X. Wan, H. Mei, Y. Liu, Y. Xu,
10 *Chem. Eur. J.* 2015, **21**, 3234; Y. M. Xie, Q. S. Zhang, Z. G. Zhao, X. Y. Wu, S. C. Chen, C. Z. Lu, *Inorg. Chem.*, 2008, **47**, 8086.

27 A. X. Tian, J. Ying, J. Peng, J.Q. Sha, Z. M. Su, H. J. Pang, P. P. Zhang, Y. Chen, M. Y. Shen, *Cryst. Growth Des.*, 2010, **10**, 1104; X. L. Wang, Y. F. Bi, B. K. Chen, H. Y. Lin, G. C. Liu, *Inorg. Chem.*, 2008,
15 **47**, 2442.

Table of contents
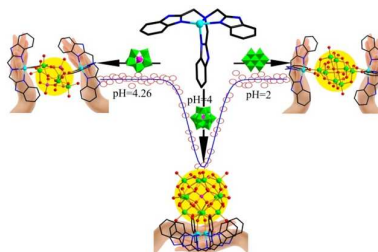
Three new polyoxometalates confined in metal-containing rigid concave surfaces are developed. All of them give a strong third-order NLO response.